REPORT DOCUMENTATION PAGE

Public reporting burden for this collection of information is estimated to average 1 hour per response, including the time for reviewing instructions, searching existing data sources, gathering and maintaining the data needed, and completing and reviewing this collection of information. Send comments regarding this burden estimate or any other aspect of this collection of information, including suggestions for reducing this burden to Department of Defense, Washington Headquarters Services, Directorate for Information Operations and Reports (0704-0188), 1215 Jefferson Davis Highway, Suite 1204, Arlington, VA 22202-4302. Respondents should be aware that notwithstanding any other provision of law, no person shall be subject to any penalty for failing to comply with a collection of information if it does not display a currently valid OMB control number. **PLEASE DO NOT RETURN YOUR FORM TO THE ABOVE ADDRESS.**

1. REPORT DATE (DD-MM-YYYY)	2. REPORT TYPE	3. DATES COVERED (From - To)
21-12-2007	Technical Paper	

4. TITLE AND SUBTITLE	5a. CONTRACT NUMBER
Analysis of Different Approaches to Modeling of the Nozzle Flows in the Near Continuum Regime (Postprint)	5b. GRANT NUMBER
	5c. PROGRAM ELEMENT NUMBER
6. AUTHOR(S)	5d. PROJECT NUMBER
E.V. Titov & D.A. Levin (Pennsylvania State University); N.E. Gimelshein & S.F. Gimelshein (ERC)	5e. TASK NUMBER 23080532
	5f. WORK UNIT NUMBER

7. PERFORMING ORGANIZATION NAME(S) AND ADDRESS(ES)	8. PERFORMING ORGANIZATION REPORT NUMBER
Air Force Research Laboratory (AFMC) AFRL/RZSA 10 E. Saturn Blvd. Edwards AFB CA 93524-7680	AFRL-RZ-ED-TP-2008-001

9. SPONSORING / MONITORING AGENCY NAME(S) AND ADDRESS(ES)	10. SPONSOR/MONITOR'S ACRONYM(S)
Air Force Research Laboratory (AFMC) AFRL/RZS 5 Pollux Drive Edwards AFB CA 93524-7048	11. SPONSOR/MONITOR'S NUMBER(S) AFRL-RZ-ED-TP-2008-001

12. DISTRIBUTION / AVAILABILITY STATEMENT

Approved for public release; distribution unlimited (PA #08001A).

13. SUPPLEMENTARY NOTES

Presented at the 46th AIAA Aerospace Sciences Meeting and Exhibit (ASME), Reno, NV, 7-10 January 2008 (AIAA 2008-750). Copyright 2008 by the American Institute of Aeronautics and Astronautics, Inc. All rights reserved.

14. ABSTRACT

A conical nozzle flow is studied for Reynolds numbers 1,230 and 12,300 using different numerical techniques: the direct simulation Monte Carlo method, the solution of Navier-Stokes equations that accounts for wall temperature jump and velocity slip, and statistical and deterministic approaches for the BGK equation. Detailed comparison of the efficiency, stability, accuracy, and convergence of the employed numerical techniques provides better understanding of their benefits and deficiencies, and assists in selecting the most appropriate technique for a particular nozzle and flow application. The deterministic solution of the BGK equation was found to be in good agreement with the benchmark DSMC results, while there were some differences observed between the statistical BGK and DSMC. The Navier-Stokes solution differs from DSMC in the boundary layer. The DSMC was shown to be the more computationally efficient than the solution of the BGK equation, both statistical and deterministic.

15. SUBJECT TERMS

16. SECURITY CLASSIFICATION OF:			17. LIMITATION OF ABSTRACT	18. NUMBER OF PAGES	19a. NAME OF RESPONSIBLE PERSON Dr. Ingrid Wysong
a. REPORT	b. ABSTRACT	c. THIS PAGE	SAR	25	19b. TELEPHONE NUMBER (include area code) N/A
Unclassified	Unclassified	Unclassified			

Standard Form 298 (Rev. 8-98)
Prescribed by ANSI Std. 239.18

Analysis of Different Approaches to Modeling of Nozzle Flows in the Near Continuum Regime

E. V. Titov * and D. A. Levin†

Pennsylvania State University, University Park, PA 16802

N. E. Gimelshein‡ and S. F. Gimelshein§

ERC, Inc., Edwards AFB, CA 93524

Conical nozzle flows are studied for Reynolds numbers of 1,230 and 12,300 using different numerical techniques: the direct simulation Monte Carlo method, Navier-Stokes/CFD that accounts for wall temperature jump and velocity slip, and statistical and deterministic approaches of the BGK equation. Detailed comparisons of the efficiency, stability, accuracy, and convergence of the employed numerical techniques provides better understanding of their benefits and deficiencies, and assists in selecting the most appropriate technique for a particular nozzle and flow application. The deterministic solution of the BGK equation was found to be in good agreement with the benchmark DSMC results, while there were some differences observed between the statistical BGK and DSMC. The Navier-Stokes solution differs from DSMC in the boundary layer.

I.   Introduction

Multiparameteric analysis of low and moderate Reynolds number nozzle flows is often problematic due to a large number of cases that need to be examined for the optimization of the nozzle-based device performance. Experimental studies under such conditions are rare, expensive, and often do not provide the necessary precision to adequately assess nozzle performance-related properties such as thrust, flow rate, and specific impulse. The problem is even worse for microscale, MEMS fabricated thrusters, whose interaction with critical spacecraft surfaces at high altitudes needs to be evaluated. Significant back flow generated by such devices plays a major role in the contamination of optical instruments, solar panels, etc. The back flow formation is very sensitive to the flow conditions at the nozzle lip, and is known to be difficult to analyze experimentally.

The development of accurate numerical tools capable of handling micronozzle flows is therefore important, although it is complicated by the change in the flow regime from continuum, near the nozzle throat,

---

*Senior research associate, Department of Aerospace Engineering, AIAA member.

†Professor, Department of Aerospace Engineering, AIAA Associate Fellow.

‡Aerospace Engineer, Edwards AFB.

§Aerospace Engineer, Edwards AFB.

American Institute of Aeronautics and Astronautics

to transitional closer to the nozzle exit plane. Both kinetic, such as the direct simulation Monte Carlo (DSMC) method, and continuum, mostly based on the solution of Navier-Stokes (N-S) equations, techniques meet computational and physical challenges when applied to these flows. The major problem with the DSMC method[1] is its often prohibitive computational cost when high density portions of the flow have to be accurately modeled. Conventional continuum CFD techniques may be inapplicable in the regions of high gradients and strong rarefaction even when the velocity slip and temperature jump corrections to the boundary conditions at the nozzle surface are used.

A combined Navier-Stokes/DSMC approach is often used in the recent years to model nozzle flows,[2,3] where the solution of the Navier-Stokes equations is used to model high density portions of the flow inside the nozzle, while the DSMC method is used to predict more rarefied plume-atmosphere interaction. A starting surface is used to hand the properties obtained in the continuum modeling off to the DSMC solver. The flow is always assumed to be in steady state, and it is implied that the more rarefied, DSMC portions of the flow have negligible effect on the upstream continuum portions. This approach becomes however not applicable when the latter implication is not true (for example, when parts of the hand-off surface are subsonic, or the downstream flow impacts the upstream flow through radiation).

In an attempt to overcome this problem, it is possible to use a two-way coupled hybrid continuum-kinetic approach (see, for example, Refs. 4–6), although, in addition of the usual hybridization problems,[7] the extantion to real gases effect or two-phase models may not be straightforward. The deficiencies of the hand-off NS-DSMC approach become even more severe when transient nozzle and plume flows need to be analyzed. In this case such an approach, as well as two-way coupled hybrid techniques, are difficult to implement. The main difficulty is related to the temporal changes in gas properties, most importantly gas mean free path and Mach number, that necessitate flexible, transient hand-off surfaces and interface boundaries.

It would therefore be highly desirable to have a single method that allows an accurate and efficient one-step modeling of high density nozzle and low density plume flows. One of the first attempts to tackle this problem was undertaken in Ref. 8 where a statistical, particle approach to the solution of the ES-BGK equation was obtained for a flow expanding through a conical nozzle. Generally, the use of a simplified form of the Boltzmann equation, usually called a model kinetic equation, such as Bhatnagar-Gross-Krook (BGK) or ellipsoidal statistical (ES-BGK) equations, may be beneficial. A method based on the solution of model kinetic equations is expected to be more efficient than the DSMC method in the continuum and near-continuum regime, and more accurate than the solution of the Navier-Stokes equations in the transitional regime.

In recent years there has been a renewed interest and significant advances in the solution of model kinetic equations, with deterministic, either finite difference or finite volume, approaches typically used in the solution procedure. A particle approach to obtain the solution to the BGK equation was first proposed in Ref. 9. It was then extended to model the ES-BGK equation in Ref. 10, and further extended to include rotational degrees of freedom in Ref. 8. The main goal of this paper is to use statistical and deterministic approaches to model kinetic equations to simulate rarefied gas flow through a conical nozzle, and compare

the results in terms of accuracy and efficiency to the DSMC method and the solution of the Navier-Stokes equations.

II. Geometry and flow conditions

Gas flow of pure argon through a conical nozzle into vacuum is considered in this work. A diverging part of the nozzle is modeled, and its geometry approximates one of the two profiles used in Ref. 11. The nozzle throat diameter is 2.5 mm, the length of the diverging part is 50.7 mm, and the half-angle is 20deg. The surface temperature of the nozzle is assumed to be 300 K. Numerical results are obtained for two throat-diameter based Reynolds numbers, 1,230 (Case I) and 12,300 (Case II), with the stagnation temperature of 333 K. In all numerical approaches, the computational domain starts at the nozzle throat and covers the entire diverging part of the nozzle, as well as a small part of the plume to avoid the influence of the downstream boundary conditions.[12] Four different numerical approaches are used, as described in the next section.

III. Computational methods

A. DSMC method

The DSMC-based SMILE computational solver was used in this work. Details on the tool may be found elsewhere.[13] The SMILE tools that were used in the present work include axisymmetric capability with radial weights, different grids for collisions and macroparameters, both of which are two-level Cartesian grids that automatically adapt to flow gradients, and parallel implementation with efficient load balancing techniques. The majorant frequency scheme was employed for modeling molecular collisions. The VHS model was used for modeling molecular interactions. Diffuse reflection with full energy accommodation was assumed on the nozzle wall. For both selected Reynolds numbers, solutions independent of grid, time step, and number of particles were obtained. For Re=1,230, there was virtually no difference observed between solutions obtained for 0.3 million cells with 1 million molecules, and 3 million cells with 10 million molecules. For Re=12,300, this was true for numerical parameters up to an order of magnitude larger.

B. Solution of NS equations

A commercial code, CFD++ has been used in this work to solve the Navier-Stokes equations. CFD++[14] is a flexible computational fluid dynamics software suite for the solution of steady and unsteady, compressible and incompressible Navier-Stokes equations, including multi-species capability for perfect and reacting gases. In this work, a perfect-gas compressible Navier-Stokes solver was used with second order spatial discretization and implicit time integration. Second order velocity slip and temperature jump conditions were imposed on the nozzle wall. A supersonic inflow with prescribed parameters were applied at the nozzle throat, and backpressure of 1 Pa was imposed at the outflow boundaries. A symmetry condition was defined at the

American Institute of Aeronautics and Astronautics

Distribution A: Approved for public release; distribution unlimited

nozzle axis. The results presented below (both flow fields and computational requirements) were obtained for a multi-block rectangular grid with a total of 14,400 nodes. The computations were also conducted for four times smaller and four times larger numbers of nodes, and found fully grid-resolved with 14,400 nodes.

C.   Finite Volume method for BGK and ES-BGK equations

A finite volume solver SMOKE developed at ERC has been used to deterministically solve the BGK and ES-BGK equations. SMOKE is a parallel code based on conservative numerical schemes developed by L. Mieussens.[15] A second order spatial discretization with axial symmetry is used along with implicit time integration. A supersonic inflow condition is used at the nozzle throat, and vacuum outflow conditions are set at the outer boundaries. Fully diffuse reflection with complete energy accommodation is applied at the nozzle surface. The spatial grid convergence was achieved increasing the number of nodes from 3,600 to over 17,000. The convergence on the velocity grid is also studied, with the number of (x, r, θ) points ranging from (20,10,18) to (30,35,50).

D.   Statistical method for BGK equation

In our earlier work,[16] we have developed and studied a statistical technique, called eDSMC, which models continuum flows through a collision enforcement procedure which guarantees full relaxation of the molecular thermal velocities to the state of local equilibrium. The technique is able to solve inviscid flows with tangency boundary conditions at the wall, but tends to under predict the viscous effects in the boundary layer when diffusional boundary conditions are used. In this work we continue our effort to apply statistical methods to moderate and high Reynolds number nozzle flows by making use of of the BGK [17] model. It is interesting to determine whether the usual DSMC method numerical requirements, that the cell size should be smaller than the local mean free path and the time step should be smaller than the mean collision time, could be substituted with standard CFD criteria such as the Currant number and the resolution of flow gradients.

Recently, a number of authors[8, 10, 18] have developed particle approaches to the solution of the BGK and ES-BGK model equations. While these approaches differ in details and theoretical arguments about the formal connection between the numerical schemes and the equations continue, the basic ideas of the numerical schemes remain the same. The essence of these kinetic approches is to select a given number of simulated particles from those available in a computational cell, and to assign to them new velocities according to the local Maxwellian (or ellipsoidal) distribution function. If the collision frequency for such a velocity reassignment is properly computed and local values of the translational temperature in the cell are known, then the procedure certainly mimics the collision term on the right hand side of the BGK equation,

$$\partial(nf)/\partial t + \mathbf{c} \cdot \partial(nf)/\partial \mathbf{r} = \nu n(f_e - f)$$

where n is the number density, ν is the collision frequency, f is the molecular velocity distribution function, f_e is the Maxwellian distribution function, $\mathbf{c}$ is the velocity vector, and $\mathbf{r}$ is the position vector.

There are arguments about the importance of certain features of the algorithms to preserve energy and momentum conservation, which in the opinion of the authors is a secondary problem, since on average these quantities are preserved. The major issue seems to be the absence of the formal derivation of the numerical schemes from the BGK equation, in a similar manner as it was conducted for DSMC schemes.[19] In this work we compare results of a statistical BGK scheme with those of the finite volume solution to the same equation. We believe that such a comparison with the results of the formally derived computational scheme can provide some insight into the features of the particle BGK scheme which we use, and probably to particle BGK schemes in general.

The details of the statistical BGK scheme are as follows. The collision frequency is calculated as

$$\nu = \text{Pr} \cdot nk \left(\frac{T_{ref}^{\omega}}{\mu_{ref}} \right) T^{\omega-1}$$

where Pr is the Prandtl number (1 for the BGK equation, in this work we used both 1 and 0.7 with no visible difference in the results), k is the Boltzmann constant, T is the translational temperature in the flow, μ_{ref} is the gas dynamic viscosity at T_{ref}. The collision frequency is calculated for each computational cell at each time step based on the local translational temperature T and the local number density n. The local number density n was averaged over a large number of computational time steps, while the local temperature T is computed based on the instantaneous velocities of the computational particles in the cell.

The number of particles in a cell preselected for velocity re-sampling was calculated as follows:

$$N_c = \text{int}(N(1 - \exp(-\nu\Delta t)))$$

where Δt is the time step, N is the number of particles in the cell and int operator means the nearest smaller integer. To compensate for the systematic error which such an operator produces, one more particle was added to to the list of preselected particles with the probability

$$P_c = N(1 - \exp(-\nu\Delta t)) - \text{int}(N(1 - \exp(-\nu\Delta t)))$$

The preselected particles received new velocities according to a Maxwellian distribution at the local cell temperature and velocity. The velocities of particles which have not been preselected remained unchanged.

Although the technique is not limited to the simple gases,[8] argon was used as the working gas in order to understand the basic features and limitations of the method without the additional complication of translational-rotational relaxation. In order to eliminate the impact of the number of particles per computational cell, a large number of particles was used so that the minimum number of particles per cell was about 150.

IV.   Results and discussion

A.   Low pressure Case I

The results presented below for the low pressure Case I were obtained by a DSMC code, its modification implementing the statistical BGK scheme, a finite volume (FV) ES-BGK solver, and a Navier-Stokes solver.

Let us first compare the results obtained by FV ES-BGK. Again, the DSMC result is assumed to the the benchmark result, since the flow condition allowed us to strictly satisfy all DSMC requirements, and the independence of the DSMC results on the parameters of the approach was verified. Figures 1 and 2 show contour plots of the translational temperature and axial velocity component, respectively, obtained by the two numerical schemes. While the general flow structure is very similar, the FV BGK scheme was found to slightly overpredict the viscous effects in the rarefied portion of the nozzle flow. This is seen both in temperature and, to somewhat larger extent, in velocity. Still, the total difference in the results obtain by different approaches is very small, and does not exceed about 3% in any portion of the flow. One possible reason for the difference may be due the difference in the collision term of the model kinetic equation and the full Boltzmann equation. The BGK and ES-BGK equations are obtained with the assumption that the collision frequency does not depend on velocities of colliding particles, and that the particles come to local equilibrium (or to the ellipsoidal distribution) after they experience $\nu\tau_c$ collisions, where ν and τ_c are the collision frequency and collision time, respectively. Note that in addition to ES-BGK, the BGK equation was also solved using a finite volume method for Case I, and the difference in the results between the BGK and ES-BGK solutions found to be within a percent.

After having established the accuracy of the FV ES-BGK scheme, let us now compare the results obtained with different approaches to the solution of model kinetic equations. Figures 3 and 4 show the contour plots of the translational temperature and axial component of velocity obtained by the deterministic and statistical approaches. The agreement is rather good in the first quarter of the nozzle, while in the remaining part the particle BGK tends to overpredict the viscous effects. For the particle solution, the axial velocity near the nozzle plane is lower, and the temperature is higher, than for the finite volume solution. The difference between the particle BGK and DSMC is even greater. Note that similar effect was observed in Ref. 8 for a diatomic gas. Possible reasons for such a difference require further investigation.

The comparison of the FV ES-BGK results with the NS predictions is given in Figs. 5 and 6. While the temperature contours are in good agreement near the nozzle centerline, there is a large difference both in translational temperature and axial velocity near the wall. The NS solution is characterized by significantly lower velocity and higher temperatures in that region, with the difference increasing toward the nozzle exit plane. The main reason for such a difference is that the velocity slip and temperature jump boundary condition used in the NS solver does not provide a correct description of gas-surface interaction, and the difference increases with the degree of thermal nonequilibrium.

An illustration of thermal nonequilibrium in the flow is provided in Fig. 7, where the ratio of the temperature in axial direction to the overall temperature is presented. In equilibrium, this ratio should be equal to the unity, and the difference from the unity serves as the measure of the flow thermal nonequilibrium. The temperature ratio presented in this figure was obtained with the DSMC method. The results show that there is a strong nonequilibrium near the nozzle lip, where the ratio is as low as 0.7. Generally, a noticeable degree of nonequilibrium exists near the nozzle wall, where the axial temperature is lower than the radial temperature, and in the middle of the nozzle off the centerline, where the radial temperature becomes larger.

The flow nonequilibrium and the difference between the translational mode temperatures indicate that the accuracy of the NS equations becomes questionable, and the may no longer be applicable. Comparison of the NS and DSMC temperature contours given in Fig. 8 clearly shows the impact of the flow nonequilibrium: there is virtually no difference between the two solutions near the nozzle axis, whereas near the nozzle wall they significantly differ.

To quantify the differences between different approaches, the gas parameters are presented along two cross sections, the nozzle centerline and the nozzle exit plane. The density, velocity, and temperature along the centerline are shown in Figs. 9-11. Here, X=0 corresponds to the nozzle throat. One of the conclusions here is that three of four our approaches produce very similar results for all gas properties under consideration. Another conclusion is that the fourth approach, namely particle BGK, produces almost 4% lower flow velocites and 25% larger gas temperatures closer to the nozzle exit plane. The reasons for the deviation needs to be investigated, here we note only that the impact of the number of particles, time step, or the cell size in the particle BGK method is unlikely to be noticeable, since the convergence of results to these parameters has been tested.

The axial velocity and temperature along the nozzle exit plane are presented in Figs. 12 and 13. Here, Y=0 corresponds to the nozzle centerline. The VF ES-BGK solution is close to that of DSMC both for the axial velocity and gas temperature. The particle BGK result agrees with the DSMC one near the wall, but start to deviate noticeably for smaller radial coordinates. The NS solver produces results accurate in the coreflow but strongly different from the ES-BGK, DSMC and particle BGK throughout the boundary layer. Generally, we can conclude that the FV ES-BGK results are in very good agreement with the DSMC in the entire diverging part of the nozzle. The solution of the model kinetic equation accurately captures both the boundary layer and the nozzle coreflow. The particle BGK results deviate from DSMC in the coreflow, and the Navier-Stokes equations appear to be inaccurate in the boundary layer.

The second most important consideration for the selection of the appropriate numerical technique for modeling nozzle flows, in addition to physical accuracy, is computational efficiency. The summary of the computational requirements necessary to complete the simulations described in this section are shown in Table 1. Note that while the CPU time given in this table represents the actual computational cost of the runs, some caution need to be used when analyzing the results. The particle simulations where conducted until the statistical scatter in major macroparameters was not visible inside the nozzle. This typically required about 10,000 timesteps to reach steady state and over 100,000 more time steps for sampling. It is of course possible to significantly reduce the number of sampling steps if larger statistical scatter is acceptable. Decreasing the number of particles is possible, but will not decrease the computational time, since a larger number of time steps for sampling will be needed. The finite volume BGK run time may be decreased by up to a factor of two without significant loss in accuracy, since it is possible to use somewhat smaller numbers of spatial cells and velocity grid points.

The results show that the Navier-Stokes solver is at least two orders of magnitude more efficient than the kinetic solvers, although its accuracy is questionable, as was illustrated earlier in this section. The DSMC

American Institute of Aeronautics and Astronautics

method is faster than the other two kinetic approaches, so for the problem under consideration the use of a BGK code does not seem to be justified. Note also that the DSMC method may requires somewhat less intervention from the user, since satisfying the usual DSMC requirements on the time step, number of particles, and cell size provides accurate results without additional convergence study. For FV ES-BGK, a convergence analysis for cell size and velocity space may be necessary unless excessively fine spatial and velocity grids are used.

B. High pressure Case II

Analysis of Case I has showed that the FV ES-BGK is comparable to the DSMC method, both in accuracy. The solution of the NS equations, while orders of magnitude more efficient, strongly underestimates flow velocity and overestimates temperature in the boundary layer. The NS equations are expected to be much more accurate for Case II, where the density is an order of magnitude larger than in Case I. At the same time the application of the DSMC method to Case II is much more time consuming, and the conventional DSMC requirements were not strictly satisfied even when over 50 million particles and 15 million cells were used. The comparison of the DSMC results obtained for smaller number of particles and cells and coarser time steps have shown however that the above DSMC parameters are sufficient for obtaining numerical parameter independent DSMC results. Significant computational difficulties were encountered when applying the FV ES-BGK to this higher density case, as several times larger number of velocity points are required to obtain grid converged results. Details about the accuracy and efficiency of the above numerical approaches are presented below.

In addition to the four approaches used to calculate Case I, the eDSMC technique[16] was also used for Case II. The collision enforcement eDSMC technique makes the flow effectively inviscid. It potentially requires less computational cells and particles and larger time steps than both DSMC and statistical BGK methods. The time step in the eDSMC technique does not depend on the local mean free path but is rather defined by the CFD type CFL number. When a boundary condition of specular reflection of computational molecules from the walls is used, eDSMC is able to properly solve the inviscid nozzle flows. In Ref.[16] it was shown that the efficiency of the baseline DSMC method could be improved when a combination of eDSMC and DSMC is applied. Although the technique underestimates the viscous effects in the boundary layer, when the diffusional boundary conditions are used, it is still capable of adequately solving the core portion of a nozzle flow.

A side-by-side comparison of the flowfields for Case II is given in Figs. 14-19. Similar to Case I, the FV ES-BGK solution is in fairly good agreement with the DSMC prediction throughout the computational domain. The particle BGK results predict velocity and temperature values similar to BGK in the downstream portion of the coreflow. However, the boundary layer is visibly thicker, and a weak compression front coming from the wall at the nozzle throat to the centerline at approximately 6 mm from the throat, predicted by both DSMC and FV ES-BGK, is not captured by particle BGK. The most probably reason for these problems is insufficient cell resolution near the nozzle wall. The solution of the NS equation is rather close to the FV

American Institute of Aeronautics and Astronautics

Distribution A: Approved for public release; distribution unlimited

ES-BGK-one, with a relatively small difference observed in the boundary layer.

A quantitative comparison of flow velocity and temperature for Case II is given in Figs. 20 and 21, where the profiles along the centerline are shown, and in Figs. 22 and 23 for the cross section along the nozzle exit plane. It is clearly seen that the DSMC, NS, and ES-BGK profiles of both velocity and temperature are very close along the nozzle centerline. The particle BGK solution deviates from the other three in the region where the compression wave comes to the centerline, and and agrees with them otherwise. The results obtained with eDSMC are similar to particle BGK in the coreflow. The results along the exit plane show that there is still some difference between the NS and DSMC predictions, both in temperature and flow velocity. As in Case I, this difference is explained by the limitations of the velocity slip boundary condition used in NS. There is also some impact of flow nonequilibrium, but its contribution is significant only near the nozzle lip, where T_x/T ration reaches 0.85. Figures 22 and 23 show that the eDSMC results are close to the results of DSMC and other methods in the core of the flow, where viscosity effect are not significant, but deviate greatly from DSMC in the boundary layer region.

The results that summarize the numerical efficiency of different approaches are shown in Table 2. The deterministic solution of the model kinetic equations becomes noticeably less efficient than the other two kinetic approaches, since a much larger number of spatial cells and velocity grid point is needed to obtain a converged result. As much as 50 angular velocity cells are necessary in this case, compared to less than 20 for Case I. It is interesting to note that computational efforts for the DSMC and statistical BGK schemes were comparable, but the convergence process was quite different. The DSMC schemes tend to converge faster, but requires more computational effort to collect the sufficient information for the solution to be smooth. Slower convergence of the statistical BGK method is probably due to the "history" of the macroparameter sampling procedure which defines the collision frequencies. This history may at the same time explain smaller statistical scatter of particle BGK. Similar to Case I, the NS solver was over two order of magnitude more efficient than the kinetic methods, however, the NS results still differ from DSMC. The eDSMC method was an order of magnitude faster than the other statistical methods, which makes it a promising statistical approach for solving the core portion of the nozzle flow in a combination with other statistical methods to proper resolve the boundary layer.

V.   Conclusions

Argon flow through a conical nozzle was studied for two Reynolds number, 1,230 and 12,300, using four different approaches. These include one continuum approach (solution of Navier-Stokes equations) and three kinetic approaches (the DSMC method and a statistical and deterministic methods for the model kinetic equations). Analyses of the accuracy of the approaches and their numerical efficiency was conducted. Several conclusion can be drawn from the results of the computations. The most accurate results in both high and low pressure cases are believed to be those obtained the DSMC method. All standard DSMC requirements were satisfied for Re=1,230. For the higher pressure case, although parameters of the numerical scheme were somewhat relaxed, a solution independent on the time step, number of simulated molecules, and cell size,

was obtained.

The Navier-Stokes solutions are in good agreement with the DSMC results in the higher density portion of the flow and in the coreflow, where rarefaction effects are small. In the boundary layer, even though the velocity slip and temperature jump boundary conditions were used, there is a difference between the NS and DSMC solutions. The finite volume solution of the ES-BGK equation is in very good agreement with the DSMC method in the entire computational domain for both Reynolds numbers. The particle BGK method agrees with the DSMC results in the boundary layer for the lower pressure case and in the coreflow for the higher pressure case. Although further analysis is needed, the deviation of the statistical BGK results from DSMC is currently attributed to the lack of formal definition of the particle BGK scheme, which may result in solutions different from the exact solution of the BGK model equation. Some of the problems in the high pressure areas of the flow can be attributed to the grid resolution, although, it was observed to be adequate in the rarefied portion of the flow where the largest difference is seen.

VI.   Acknowledgments

References

[1]Bird, G. A., *Molecular Gas Dynamics and the Direct Simulation of Gas Flows*, Clarendon Press, Oxford, 1994.

[2]Gimelshein, S., Alexeenko, A., and Levin, D., "Modeling of the interaction of a side jet with a rarefied atmosphere." *Journal of Spacecraft and Rockets*, Vol. 39, No. 2, 2002, pp. 168–176.

[3]Gimelshein, N., Lyons, R., Reuster, J., and Gimelshein, S., "Numerical Prediction of UV Radiation from Two-Phase Plumes at High Altitudes," .

[4]Eggers, J., "New algorithms for application in the direct simulation Monte Carlo method," *In Rarefied Gas Dynamics: Theory and Simulations, ed. BD Shizgal, DP Weaver, Progress in Astronautics and Aeronautics*, Vol. 159, pp. 166–173.

[5]Roveda, R., Goldstein, D., and Varghese, P., "Hybrid Euler/particle approach for continuum/rarefied flows," *J Spacecraft Rockets*, 1998, pp. 258–265.

[6]Arslanbekov, J. R., Kolobov, V., and Gimelshein, S., "Testing of the Unified Flow Solver (UFS) for Nozzle and Plume Flows," .

[7]Bourgat, J., Tallec, P., and Tidriri, M., "Coupling Boltzmann and Navier-Stokes Equations by friction," *Journal of Computational Physics*, , No. 127, 1996, pp. 227–245.

[8]Burt, J. M. and Boyd, I. D., "Evaluation of a Particle Method for the Ellipsoidal Statistical Bhatnagar-Gross-Kroook Equation," *44th AIAA Aerospace Science Meeting and Exhibit, AIAA Paper 2006-989, Reno, Nevada*, January 2006.

[9]Nanbu, K., Igarashi, S., and Watanabe, Y., "Stochastic solution method of the model kinetic equation for diatomic gas," *Journal of the Physical Society of Japan*, pp. 3371–3375.

American Institute of Aeronautics and Astronautics

Distribution A: Approved for public release; distribution unlimited

[10]Gallis, M. A. and Torczynski, J. R., "The Application of the BGK Model in Particle Simulations," *AIAA Paper No. 2000-2360, 34th AIAA Thermophysics Conference, Denver Co.*, June 2000.

[11]Rothe, D. E., "Electron-Beam Studies of Viscous Flows in Supersonic Nozzles," *AIAA Journal*, Vol. 9, 1971, pp. 809–811.

[12]Ivanov, M., Markelov, G., Ketsdever, A., and Wadsworth, D., "Numerical Study of Cold Gas Micronozzle Flows," .

[13]Ivanov, M. and Gimelshein, S., "Current Status and Prospects of the DSMC Modeling of Near-Continuum Flows of Non-reacting and Reacting Gases," *Proceedings of the Rarefied Gas Dynamics 23rd Int. Symp., AIP Conference*, Vol. 663, 2003, pp. 339–348.

[14]"CFD++ User Manual Version 5.1.1," 2005.

[15]Mieussens, L., "Discrete-Velocity Models and Numerical Schemes for the Boltzmann-BGK Equation in Plane and Axisymmetric Geometries," *Journal of Computational Physics*, Vol. 162, 2000, pp. 429–466.

[16]E.V.Titov and D.A., "Extension of the DSMC method to high pressure flows," *Journal of Computational Fluid Dynamics*, Vol. 21, 2007, pp. 351.

[17]Bhatnagar, P., Gross, E., and Krook, M., "A model for collision processes in gases," *Physical Review*, Vol. 94, 1954, pp. 511.

[18]Macrossan, M., "A Particle Simulation Method for the BGK Equation," *Proceedings of the 22 International Symposium on Rarefied Gas Dynamics*, 2001, pp. 426–433.

[19]Ivanov, M. and Rogasinsky, S., "Analysis of numerical techniques of the direct simulation Monte Carlo method in the rarefied gas dynamics," *Soviet Journal of Numerical Analysis and Mathematical Modeling*, Vol. 3, 1988, pp. 453–465.

American Institute of Aeronautics and Astronautics

Table 1. Parameters of the methods, Case I

Method	DSMC	Part BGK	FV ES-BGK	NS
Time (CPUH)	200	1000	400	<1
Number of particles	10 mil	50 mil	-	-
Number of cells	3 mil	0.5 mil	3,600	3,600

Table 2. Parameters of the methods, Case II

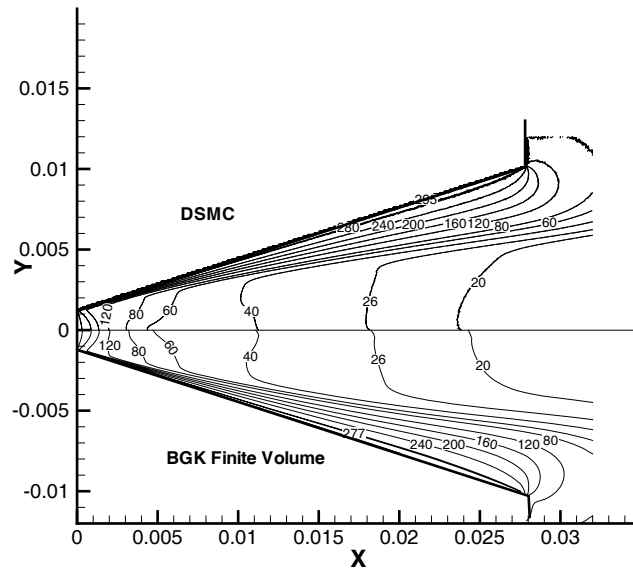| Method	DSMC	Part BGK	FV ES-BGK	NS	eDSMC
Time (CPUH)	1000	1000	5000	3	100
Number of particles	50 mil	50 mil	-	-	1 mil
Number of cells	15 mil	0.5 mil	17,200	14,400	100,000
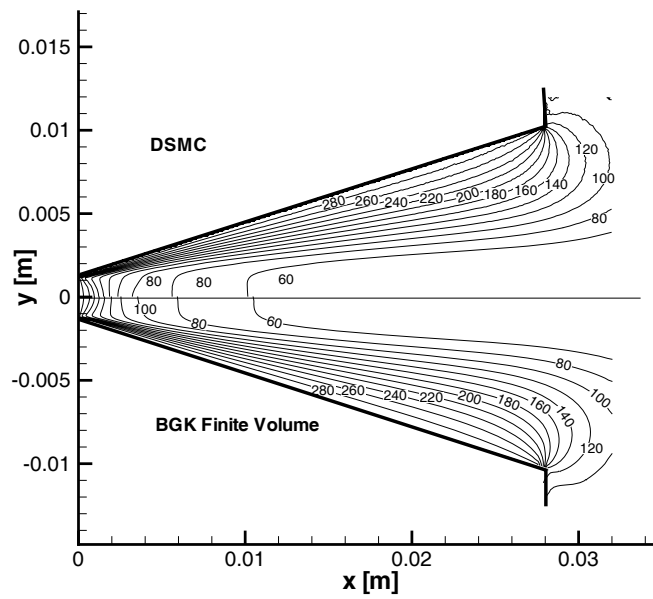
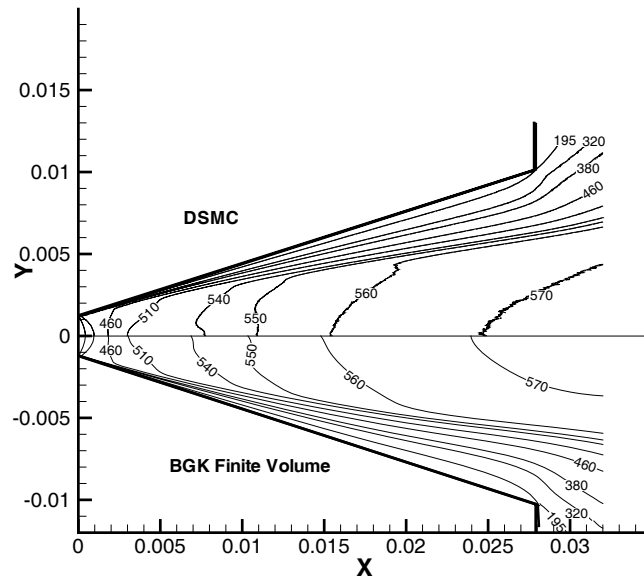Figure 1. Case I, DSMC and FV ES-BGK temperature contours (K).
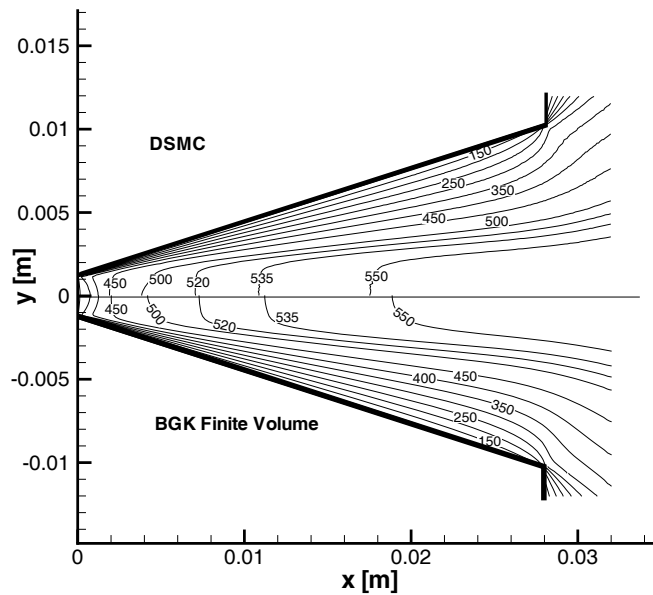
Figure 2. Case I, DSMC and FV ES-BGK axial velocity contours (m/s).
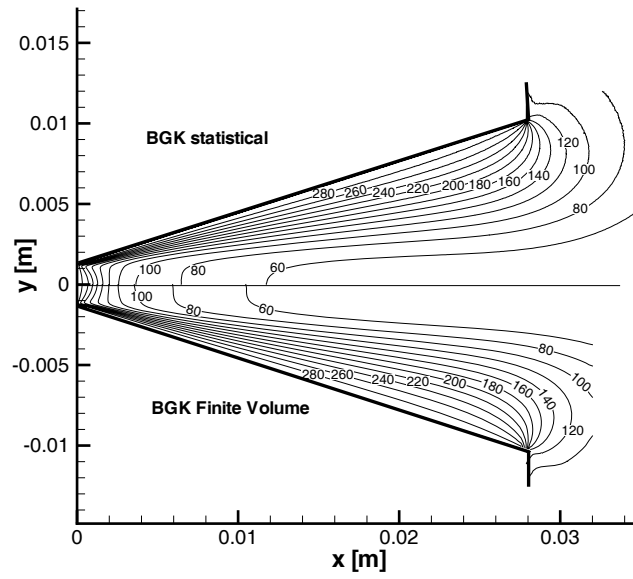
Figure 3. Case I, Particle BGK and FV ES-BGK temperature contours (K).
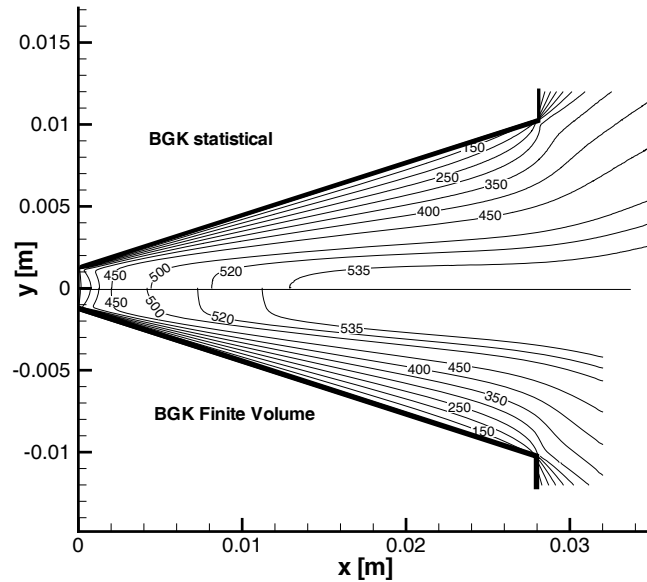
Figure 4. Case I, Particle BGK and FV ES-BGK axial velocity contours (m/s).

American Institute of Aeronautics and Astronautics
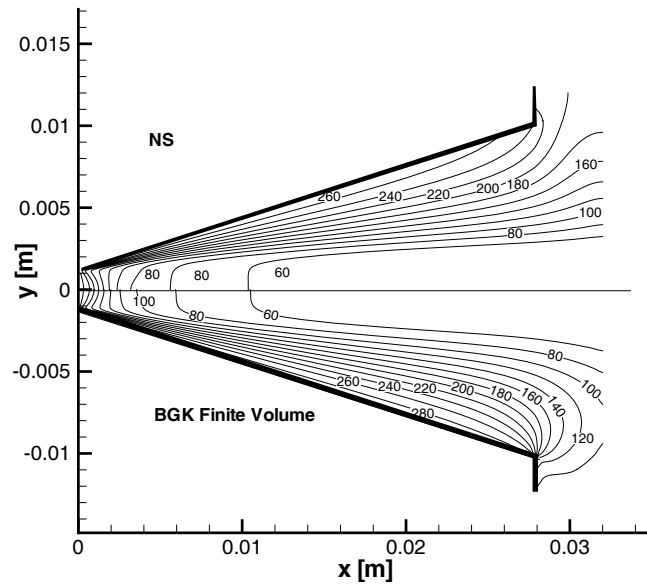
Figure 5. Case I, NS and FV ES-BGK temperature contours (K).
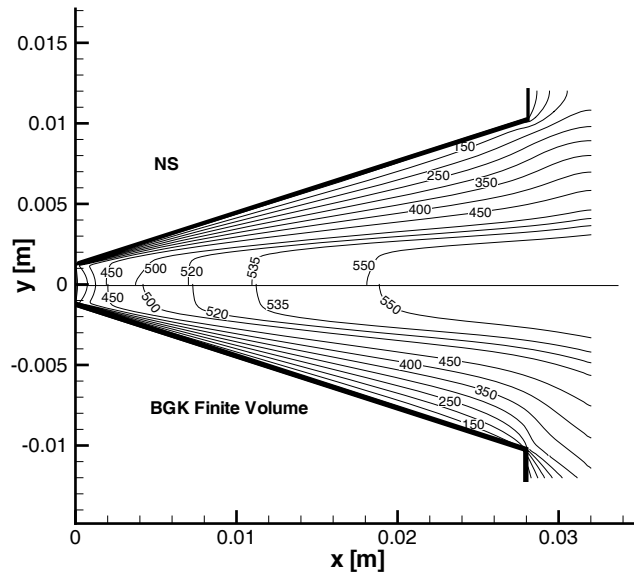
Figure 6. Case I, NS and FV ES-BGK axial velocity contours (m/s).

American Institute of Aeronautics and Astronautics
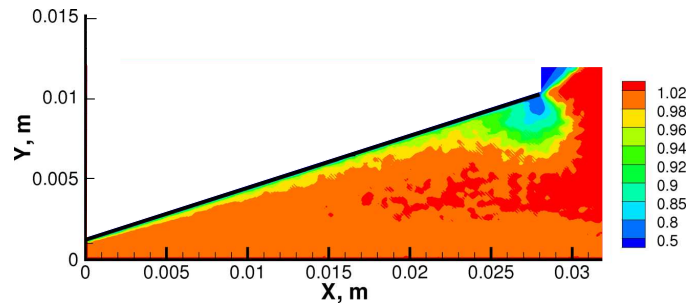
Figure 7. Case I, DSMC T_x/T ratio.
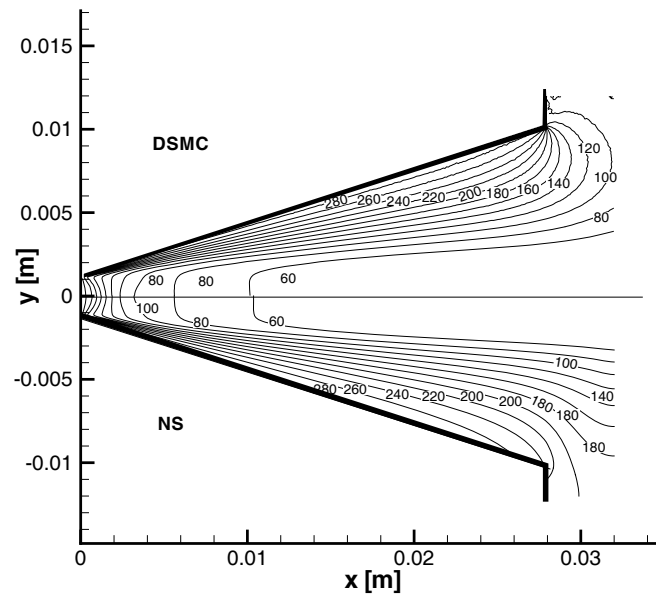
Figure 8. Case I, DSMC and NS temperature contours (K).

American Institute of Aeronautics and Astronautics
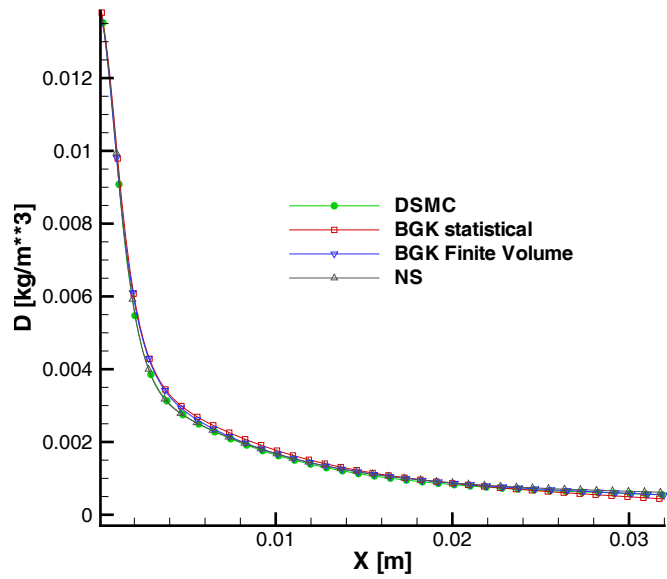
Figure 9. Case I, Density along the centerline.
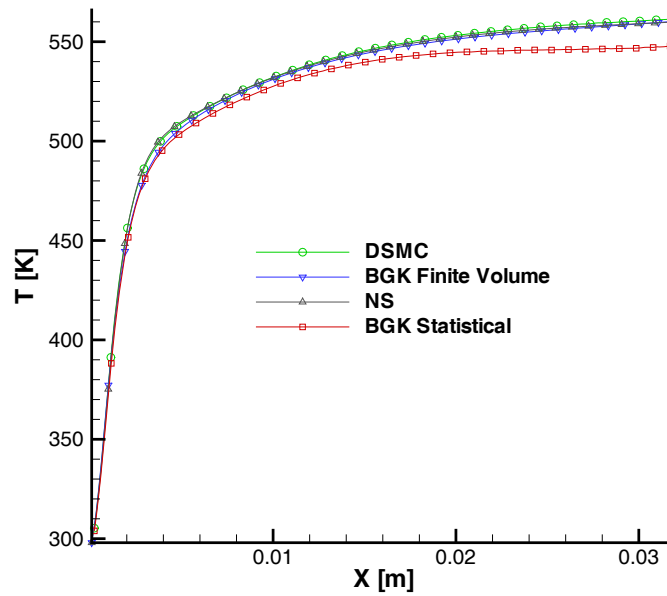
Figure 10. Case I, Axial velocity along the centerline.
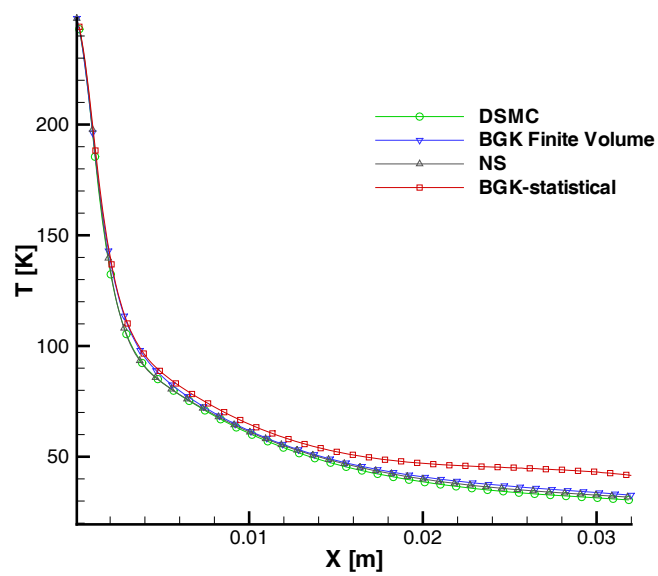
Figure 11. Case I, Temperature along the centerline.

American Institute of Aeronautics and Astronautics
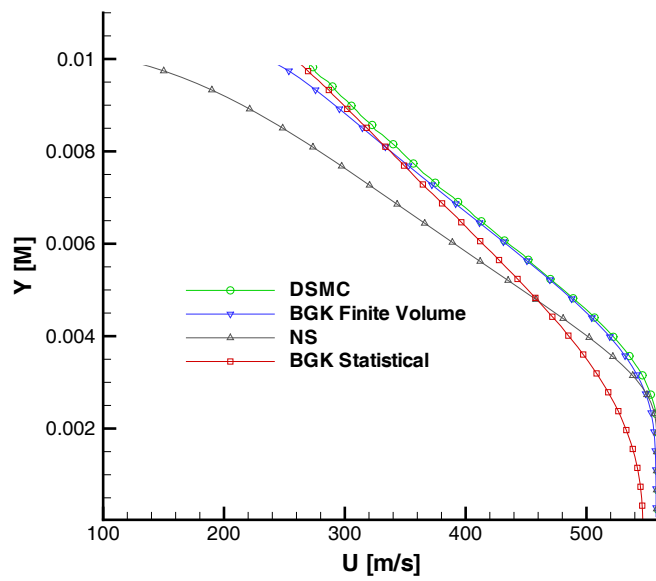
Figure 12. Case I, Axial velocity at the nozzle exit.
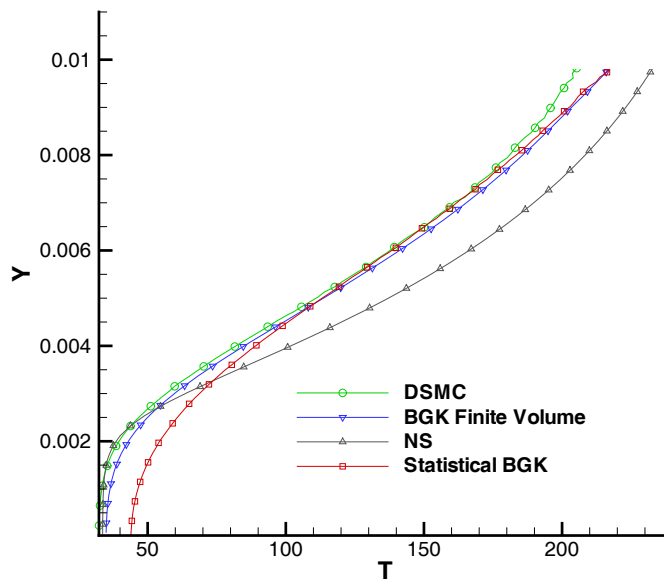
Figure 13. Case I, Temperature at the nozzle exit.

American Institute of Aeronautics and Astronautics

Figure 14. Case II, DSMC and FV ES-BGK temperature contours (K).

Figure 15. Case II, DSMC and FV BGK axial velocity contours (m/s).
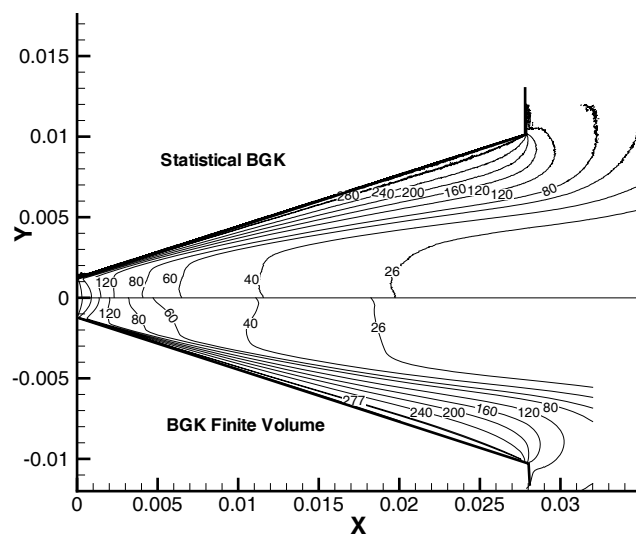
Figure 16. Case II, Particle BGK FV ES-BGK temperature contours (K).
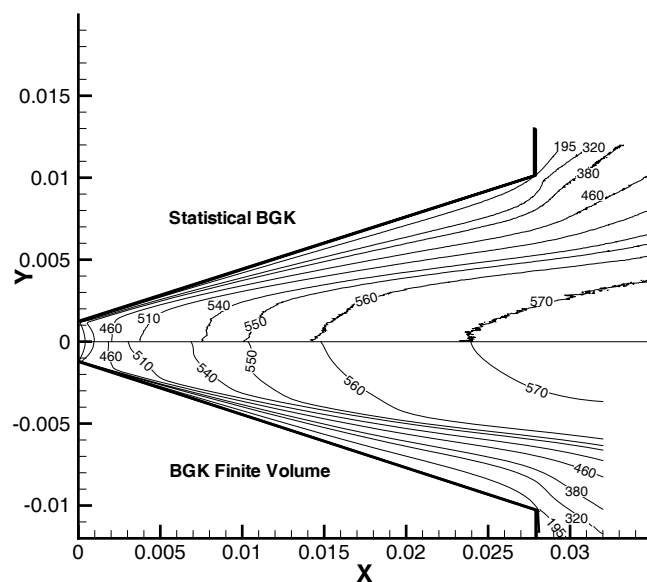
Figure 17. Case II, Paricle and FV BGK axial velocity (m/s).

American Institute of Aeronautics and Astronautics
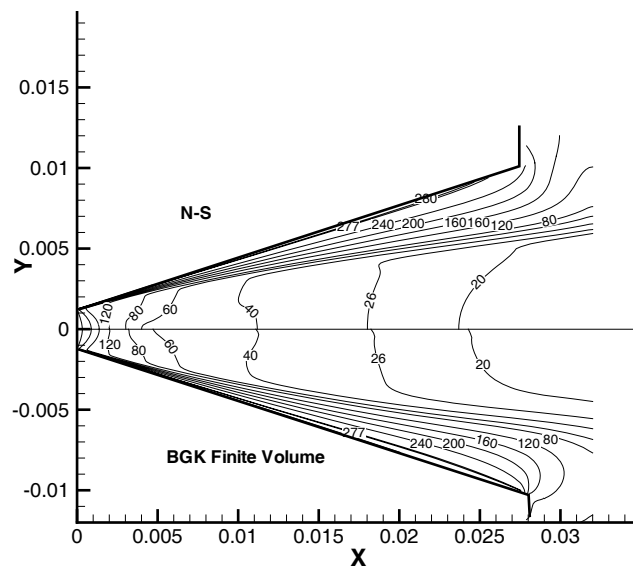
Figure 18. Case II, NS and FV ES-BGK temperature contours (K).
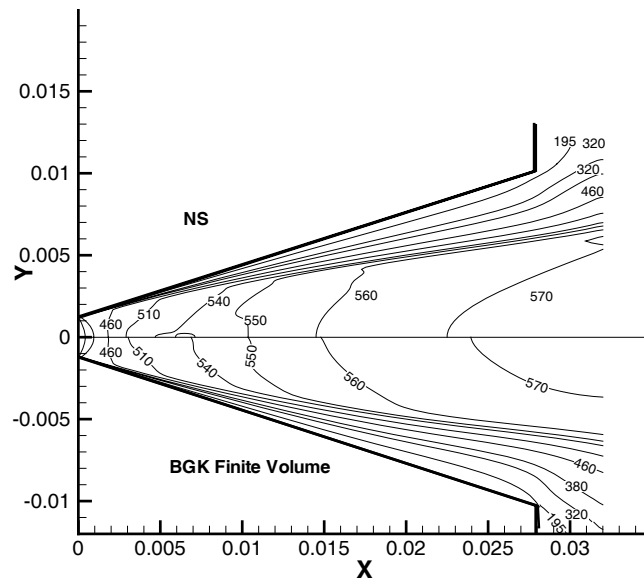
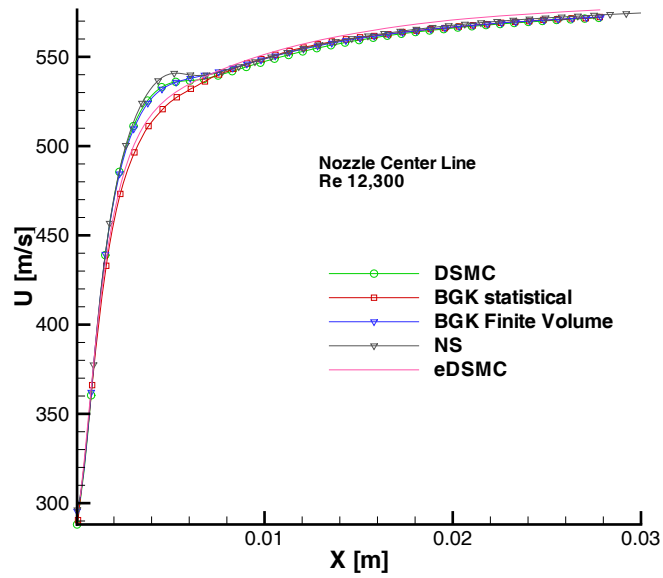Figure 19. Case II, NS and FV ES-BGK axial velocity contours (m/s).

American Institute of Aeronautics and Astronautics

Figure 20. Case II, Axial velocity along the centerline.
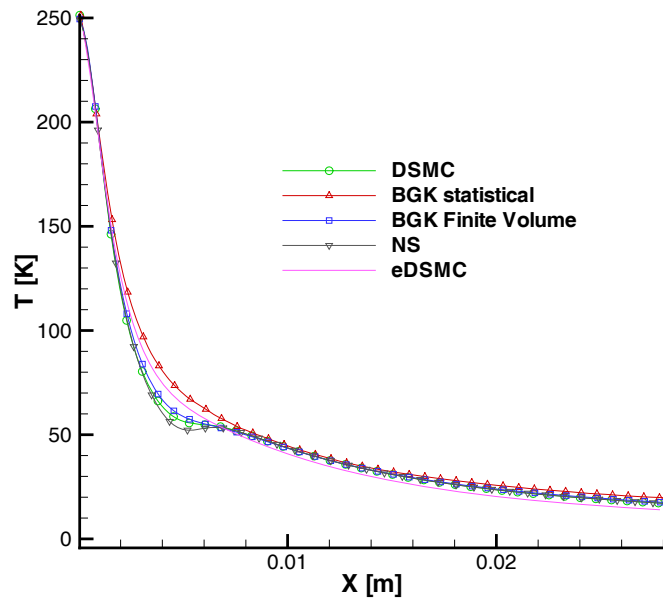
Figure 21. Case II, Temperature along the centerline.

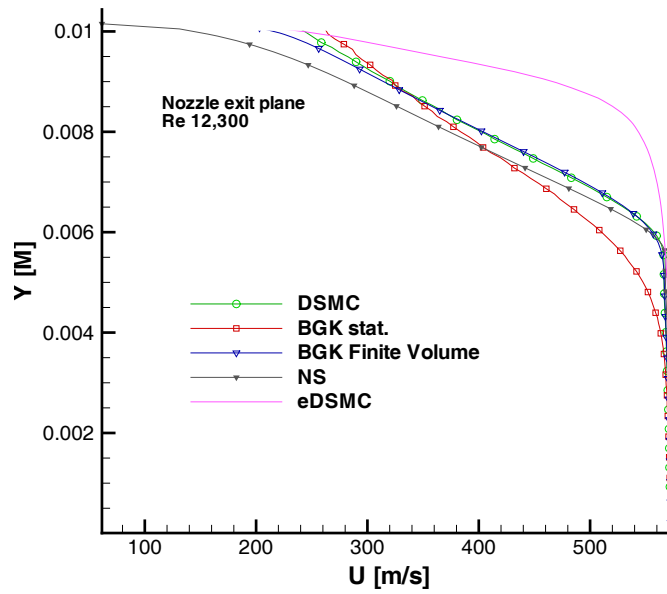American Institute of Aeronautics and Astronautics
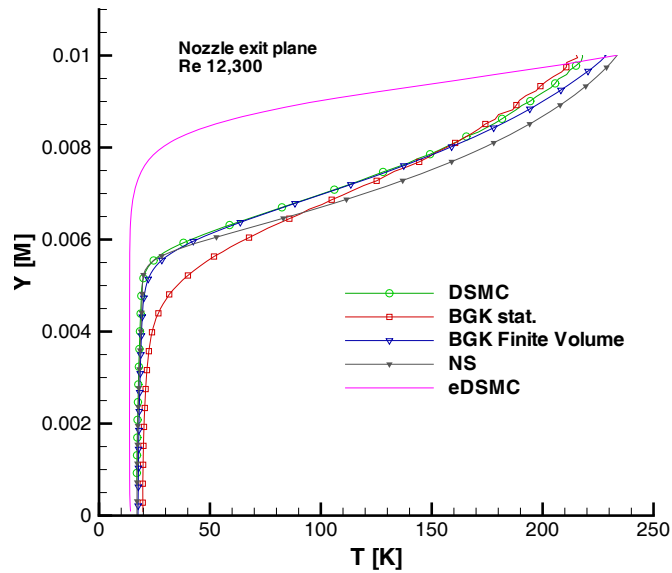
Figure 22. Case II, Axial velocity at the nozzle exit.

Figure 23. Case II, Temperature at the nozzle exit.

American Institute of Aeronautics and Astronautics